Short communication

Effects of fluorine-substitution on the electrochemical behavior of LiFePO$_4$/C cathode materials

Xiao-Zhen Liao, Yu-Shi He, Zi-Feng Ma*,
Xiao-Ming Zhang, Liang Wang

*Department of Chemical Engineering, Shanghai Jiao Tong University,
Shanghai 200240, People's Republic of China*

Available online 28 June 2007

Abstract

The effects of fluorine substitution on the electrochemical properties of LiFePO$_4$/C cathode materials were studied. Samples with stoichiometric proportion of LiFe(PO$_4$)$_{1-x}$F$_{3x}$/C ($x = 0.025, 0.05, 0.1$) were prepared by adding LiF in the starting materials of LiFePO$_4$/C. XRD and XPS analyses indicate that LiF was completely introduced into bulk LiFePO$_4$ structure in LiFe(PO$_4$)$_{1-x}$F$_{3x}$/C ($x = 0.025, 0.05$) samples, while there was still some excess of LiF in LiFe(PO$_4$)$_{0.9}$F$_{0.3}$/C sample. The results of electrochemical measurement show that F-substitution can improve the rate capability of these cathode materials. The LiFe(PO$_4$)$_{0.9}$F$_{0.3}$/C sample showed the best high rate performance. Its discharge capacity at 10 C rate was 110 mAh g^{-1} with a discharge voltage plateau of 3.31–3.0 V versus Li/Li$^+$. The LiFe(PO$_4$)$_{0.9}$F$_{0.3}$/C sample also showed obviously better cycling life at high temperature than the other samples.
© 2007 Elsevier B.V. All rights reserved.

Keywords: Fluorine substitution; Lithium ion phosphate; Cathode materials

1. Introduction

Lithium ion phosphate LiFePO$_4$ has attracted great attention as a promising replacement for LiCoO$_2$ because of its low cost, low toxicity and safety [1,2]. However, a main drawback of pristine LiFePO$_4$ is its very low intrinsic electronic conductivity, which results in poor rate performance. To solve this problem, various methods have been applied. The most successful approaches are cation substitution [3], particle size reduction [4–6] and carbon coating at the surface of LiFePO$_4$ particles [7–13]. Anion substitution, on the other hand, is less often attempted.

Fluorine substitution at the oxygen site of the cathode active materials for lithium ion batteries attracts much attention in recent years [14–16]. It is reported that the fluorine substitution is effective to improve cycling life for layered structure cathode materials. The crystal structure of these materials was stabilized by partially substituting fluorine for oxygen, and the phase transitions during charge and discharge are partially suppressed [17–19]. Sun and co-workers [20–22] reported that F doping at the oxygen site of LiNiO$_2$ and Li[Ni$_{1/3}$Co$_{1/3}$Mn$_{1/3}$]O$_2$ can improve high rate capability and cycle stability, even at high upper voltage limit of 4.6 V. Furthermore, fluorine substitution catalyzes the growth of the primary particles, which in turn results in high tap density as well as high volumetric capacity. Amatucci et al. [23] observed that fluorine doping at the oxygen site of LiAl$_{0.2}$Mn$_{1.8}$O$_{3.8}$F$_{0.2}$ resulted in improvements in capacity and its retention during 300 cycles, and exhibited enhanced stability at elevated temperature. They attributed these beneficial effects to the resistance of fluorides to attack by HF found in the electrolyte. A novel lithium vanadium fluorophosphate, LiVPO$_4$F, was synthesized by Valence Technology [24], its electrochemical insertion properties was studied. It indicated that the V^{3+}/V^{4+} redox couple in LiVPO$_4$F is located at a potential around 0.3 V higher than that for the same transition in the lithium vanadium phosphate, Li$_3$V$_2$(PO$_4$)$_3$. This property characterizes the impact of structural fluorine on the inductive effect of the PO$_4^{3+}$ polyanion. All of the results mentioned above show the positive effects of fluorine on the cathode materials for lithium ion batteries. However, fewer reports on fluorine substitution for LiFePO$_4$ materials have been issued. In this work, a series of F-substituted LiFe(PO$_4$)$_{1-x}$F$_{3x}$/C ($x = 0.025$,
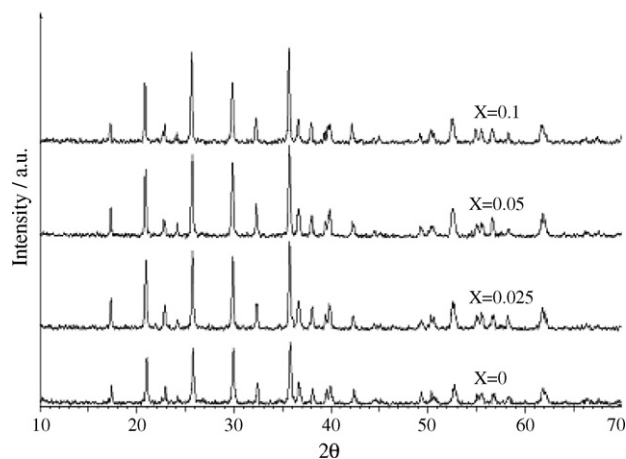
Fig. 1. X-ray diffraction patterns of LiFe$(PO_4)_{1-x}F_{3x}$/C ($x = 0, 0.025, 0.05, 0.1$).

0.05, 0.1) cathode materials were synthesized to investigate the effects of fluorine substitution on the electrochemical properties of LiFePO$_4$/C.

2. Experimental

LiFe$(PO_4)_{1-x}F_{3x}$/C ($x = 0, 0.025, 0.05,$ and 0.1) samples were synthesized by using a ball milling procedure according to the following reaction equation:

$$Fe + 2FePO_4 \cdot 4H_2O + (1 - 3x)Li_3PO_4 \cdot \tfrac{1}{2}H_2O + 9xLiF$$
$$\rightarrow 3LiFe(PO_4)_{1-x}F_{3x} + (17 - 3x)/2H_2O$$
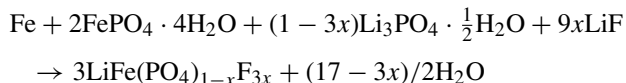
Sucrose was added as a conductive additive precursor in the starting mixture. The products of ball milling were heat-treated at 600–650 °C for 30 min to obtain the final LiFe$(PO_4)_{1-x}F_{3x}$/C ($x = 0$, 0.025, 0.05, and 0.1) samples with a carbon content about 2.7 wt.%. The synthesis procedure is the same as that of LiFePO$_4$/C as described in detail elsewhere [12,13], except partly replacement of Li$_3$PO$_4$·1/2H$_2$O with LiF in the starting mixture based on the above reaction equation.

Powder X-ray diffraction (XRD) measurements were carried out over the 2θ range from 10° to 70° with a Philips 3100E diffract meter using Cu Kα radiation ($\lambda = 1.54$ Å). The binding energy of fluorine ion was investigated by X-ray pho-

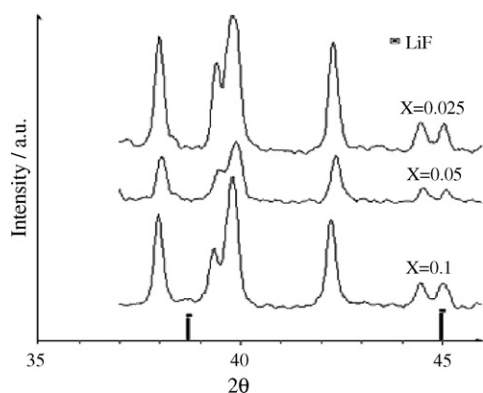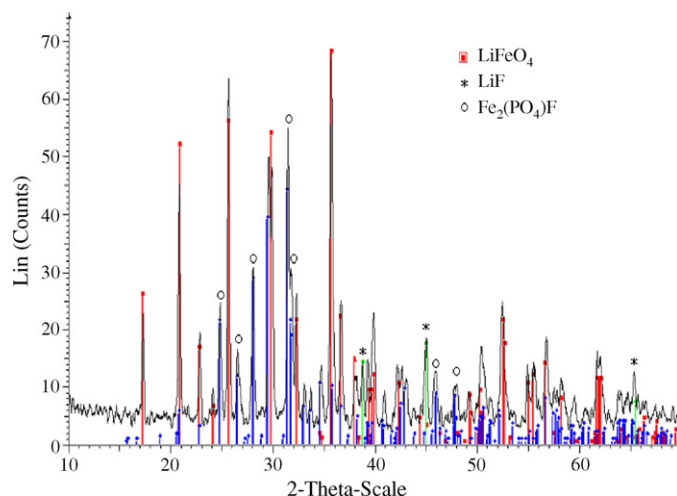Fig. 3. X-ray diffraction pattern of the product using LiF as lithium source instead of Li$_3$PO$_4$.

toelectron spectroscopy (XPS). XPS spectra were collected on a PHI-5000C ESCA system (Perkin-Elmer) with Al Kα radiation (1486.6 eV), the base pressure of the analyzer chamber was about 5×10^{-7} Pa, and the binding energies were calibrated by using the containment carbon (C$_{1s}$ = 284.6 eV). The electrochemical characteristics of the LiFe$(PO_4)_{1-x}F_{3x}$/C ($x = 0$, 0.025, 0.05, 0.1) samples were measured by using a R2016 button cell. A composite electrode consisting of 75 wt.% active material, 15 wt.% acetylene black and 10 wt.% PVDF binder was used as positive electrode. A lithium metal foil was used as anode. LiPF$_6$ (1 M) in a 1:1(v/v) mixture of dimethyl carbonate (DMC) and ethylene carbonate (EC) was used as electrolyte. Charge–discharge performances were evaluated using a battery test system (LAND CT2001A model, Wuhan Jinnuo Electronics Co., Ltd.) under a constant current condition.

3. Results and discussion

Fig. 1 shows the XRD patterns for the prepared LiFe $(PO_4)_{1-x}F_{3x}$/C ($x = 0$, 0.025, 0.05, 0.1) samples. The diffraction peaks of the F-substituted materials were almost the same as the peaks of LiFePO$_4$/C with an ordered olivine structure
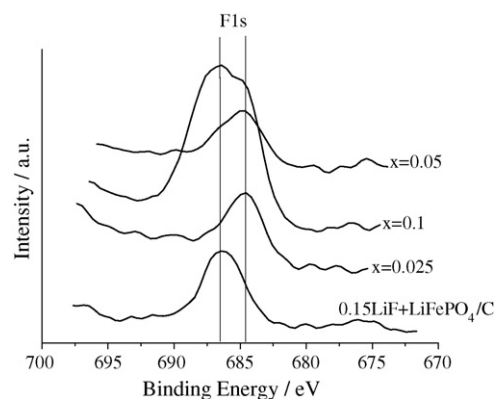

Fig. 2. X-ray diffraction patterns of LiFe$(PO_4)_{1-x}F_{3x}$/C ($x = 0.025, 0.05, 0.1$) in the 2θ range of 37–46°.

Fig. 4. F$_{1s}$ XPS spectra of LiFe$(PO_4)_{1-x}F_{3x}$/C ($x = 0.025, 0.05, 0.1$) samples and 0.15LiF + LiFePO$_4$/C mixture.
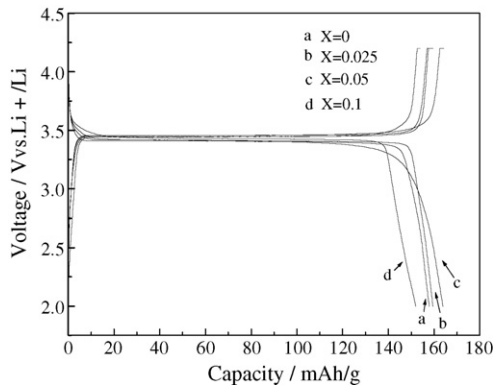
Fig. 5. Tenth charge–discharge curves of the LiFe(PO$_4$)$_{1−x}$F$_{3x}$/C (x = 0, 0.025, 0.05, 0.1) samples at 0.1 C rate.

indexed to the orthorhombic *Pnmb* space group. A very slightly shift to the lower 2θ angle of the diffraction peaks for the F substituted materials was observed as the F content increased, the relative intensities of the peaks changed. This indicates that F was successfully introduced into LiFePO$_4$ matrix structure and the incorporation of F did not alter the LiFePO$_4$ structure but slightly increased the lattice parameters.

In order to clarify whether the added LiF in the starting materials was all introduced into the LiFePO$_4$ matrix structure, the fine structures of LiFe(PO$_4$)$_{1−x}$F$_{3x}$/C (x = 0.025, 0.05, 0.1) samples in the 2θ range of 37–46° were detected as shown in Fig. 2. It can be seen that the XRD pattern of LiFe(PO$_4$)$_{0.9}$F$_{0.3}$/C includes a weak peak at 2θ = 38.7°, which is a typical of LiF. No diffraction peaks from LiF were identified for LiFe(PO$_4$)$_{1−x}$F$_{3x}$/C (x = 0.025, 0.05) samples. However, what happen to fluorine during the mechaochemical reaction? In order to clarify this question, we prepared a special sample by entirely using LiF instead of Li$_3$PO$_4$ as lithium source. The molar ratio of the starting mixture was LiF:FePO$_4$·4H$_2$O:Fe = 3:2:1. Fig. 3 shows the XRD pattern of the resulting product. XRD analysis showed that the resulting powder was a mixture of LiFePO$_4$, Fe$_2$(PO$_4$)F and LiF. From these results we assume that the fluorine was introduced into the bulk of lithium ion phosphate by substitution of F$^−$ for PO$_4{}^{3−}$ in the F-substituted LiFe(PO$_4$)$_{1−x}$F$_{3x}$/C (x = 0.025, 0.05, 0.1) samples.

The XPS spectra of F$_{1s}$ for LiFe(PO$_4$)$_{1−x}$F$_{3x}$/C (x = 0.025, 0.05, 0.1) samples and the LiFePO$_4$/C + 0.15LiF mixture were illustrated in Fig. 4, respectively. It can be found that both LiFe(PO$_4$)$_{0.95}$F$_{0.15}$/C and LiFe(PO$_4$)$_{0.975}$F$_{0.075}$/C samples exhibited one F$_{1s}$ peak centered at 684.59 eV, which is different from the peak position of LiF (686.52 eV) in the LiFePO$_4$/C + 0.15LiF mixture. The F$_{1s}$ peak around 684.59 eV may be attributed to the F–Fe bond. On the other hand, there are obviously two F$_{1s}$ peaks at 684.59 and 686.52 eV for LiFe(PO$_4$)$_{0.9}$F$_{0.3}$/C sample. The LiFe(PO$_4$)$_{0.9}$F$_{0.3}$/C sample was over-substituted and some excess LiF was detected. These results consist with the XRD analyses.

Fig. 5 presents the charge–discharge voltage profiles of the Li|LiFe(PO$_4$)$_{1−x}$F$_{3x}$/C (x: 0, 0.025, 0.05, 0.1) cells between 2.0 and 4.2 V using a low constant current density of 17 mA g^{-1}. Fluorine substitution did not change the potential profile of
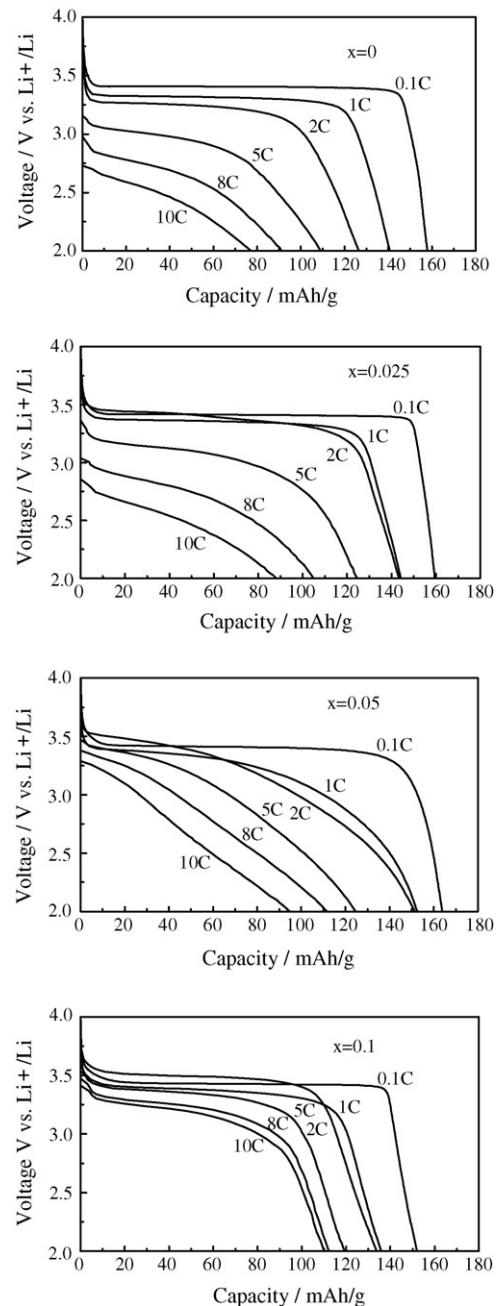

Fig. 6. Discharge profiles of the LiFe(PO$_4$)$_{1−x}$F$_{3x}$/C (x = 0, 0.025, 0.05, 0.1) samples at various C rates. Charge rate 0.1 C.

LiFePO$_4$/C. Slightly substitution increased the reversible capacity of substituted materials. However, heavy substitution caused a capacity loss. The LiFe(PO$_4$)$_{0.9}$F$_{0.3}$/C sample delivered a lower discharge capacity of 151.6 mAh g^{-1} compared to 159.4, 163.88 and 157.9 mAh g^{-1} for LiFe(PO$_4$)$_{1−x}$F$_{3x}$/C (x = 0.025, 0.05, 0), respectively. The lithium ions corresponding to the excess LiF in the LiFe(PO$_4$)$_{0.9}$F$_{0.3}$/C sample did not contribute to charge/discharge capacity of the cathode material.

Fig. 6 compares the rate performance of LiFe(PO$_4$)$_{1−x}$F$_{3x}$/C (x = 0, 0.025, 0.05, 0.1) samples. The discharge curves were tested at various C rates. The cut-off voltage was 2.0 V. The cells were recharged at 0.1 C rate (17 mA g^{-1}). It can be seen
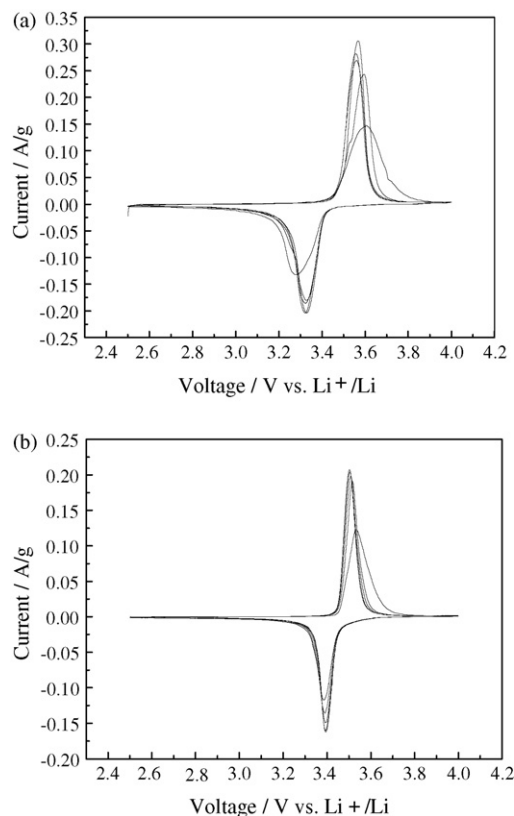
Fig. 7. Cyclic voltammograms of (a) Li|LiFePO$_4$/C and (b) Li|LiFe(PO$_4$)$_{0.9}$F$_{0.3}$/C cells at a scan rate of 0.05 mV s^{-1}.

that the discharge performance of un-substituted LiFePO$_4$/C was strongly affected by C rate. The average discharge voltage decreased obviously from 3.4 V (0.1 C) to 3.0 V (5 C) with increased C rate. On the other hand, F substituted samples show increased initial discharge voltage at all test current densities, and the drop of initial discharge voltage with the increased C rate was alleviated. This suggests that F-substitution could improve the electric conductivity of these cathode materials, which alleviated the polarization of the active materials under high current densities. The heavily F substituted LiFe(PO$_4$)$_{1-x}$F$_{3x}$/C ($x = 0.1$) sample exhibited very attractive behavior. Although the primary capacity was lower than the other samples, it showed much better capacity retention as discharge current density increased. It can also be seen from Fig. 6 ($x = 0.1$) that LiFe(PO$_4$)$_{0.9}$F$_{0.3}$/C sample exhibited the best high rate performance. As the discharge current density increased, the average voltage of the discharge profiles only slightly decreased from 3.428 V (0.1 C) to 3.35 V (5 C) and 3.20 V (10 C). Furthermore, all its high rate discharge profiles displayed good flat plateaus. The discharge capacities at different C rates were 151.9 mAh g^{-1} (0.1 C), 119.4 mAh g^{-1} (5 C) and 109.8 mAh g^{-1} (10 C), respectively. These results indicate that the diffusion of lithium ions was improved by F-substitution. The high ionicity of F$^-$ may contribute to the motion of lithium ion in the F-substituted materials.

The effects of fluorine substitution on the electrochemical performance of LiFePO$_4$/C materials can be further understand by cyclic voltammograms. Fig. 7 shows the CV curves of Li|LiFePO$_4$/C and Li|LiFe(PO$_4$)$_{0.9}$F$_{0.3}$/C cells measured

between 2.5 and 4.0 V at a scan-rate of 0.05 mV s^{-1}. The two samples show similar CV curves with one pair of redox peak. The redox peaks of LiFe(PO$_4$)$_{0.9}$F$_{0.3}$/C and LiFePO$_4$/C samples were centered at 3.507/3.395 and 3.560/3.327 V, respectively. It is noticed that the peak separation of LiFe(PO$_4$)$_{0.9}$F$_{0.3}$/C sample is narrower and the peak shape was shaper than LiFePO$_4$/C. This result indicates an easier lithium insertion and extraction in the fluorine substitution samples.

Fig. 8 presents the cycling characteristics of the LiFe(PO$_4$)$_{1-x}$F$_{3x}$/C ($x = 0$, 0.025, 0.05, 0.1) cathode materials at 25 and 55 °C. The cells were cycled between 2.0 and 4.2 V at 1 C charge–discharge rate. A comparison of these profiles is easy to find that the cycle stability of LiFe(PO$_4$)$_{0.95}$F$_{0.15}$/C and LiFe(PO$_4$)$_{0.975}$F$_{0.075}$/C samples is similar to that of un- substituted LiFePO$_4$/C at both 25 and 55 °C. The fully F-substituted LiFe(PO$_4$)$_{0.9}$F$_{0.3}$/C sample exhibited obviously better cycle life than the other samples, especially at elevated temperature. The cycling profiles tested at 55 °C (Fig. 8b) show that LiFe(PO$_4$)$_{1-x}$F$_{3x}$/C ($x = 0$, 0.025, 0.05) samples all delivered an initial discharge capacity large than 160 mAh g^{-1} at 55 °C, however, the capacity fade obviously after 100 cycles. The capacity of the 300th cycle for these samples was 107.3, 109.8 and 106.9 mAh g^{-1}, respectively, which was less than 70% of their initial capacities. On the other hand, while the initial discharge capacity of LiFe(PO$_4$)$_{0.9}$F$_{0.3}$/C was 155.7 mAh g^{-1}, it demonstrated improved cycling performance and only 2.5% capacity fade was observed after 200 cycles. It still remained a capacity of 143.1 mAh g^{-1} at the 300th cycle, which was 91.8% of its initial capacity. In order to
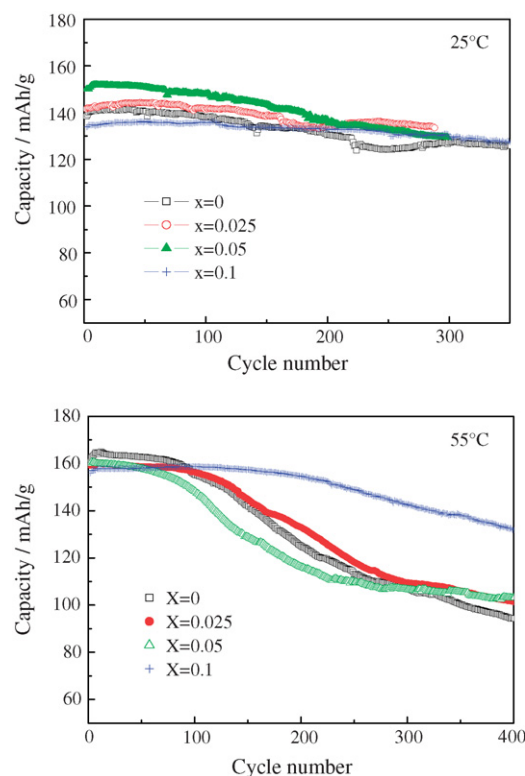

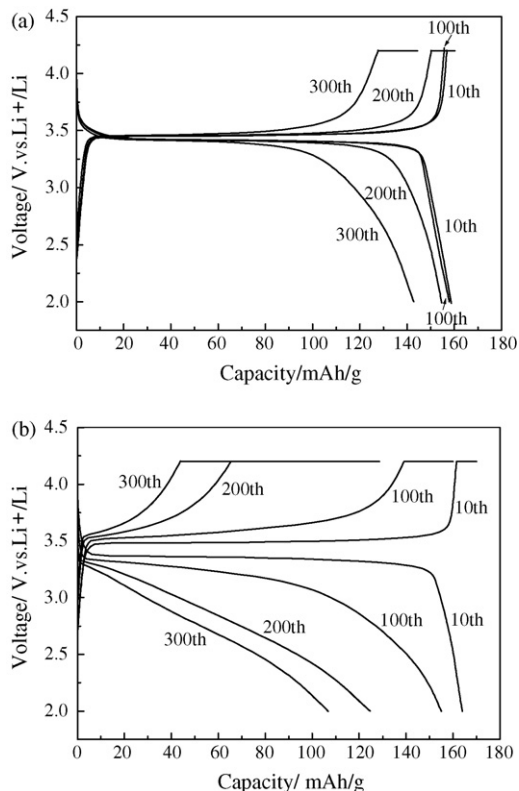Fig. 8. Cycling performance Li|LiFe(PO$_4$)$_{1-x}$F$_{3x}$/C ($x = 0$, 0.025, 0.05, 0.1) cells at 1 C charge–discharge rate.

Fig. 9. Charge–discharge profiles at 55 °C under 1 C rate for (a) LiFePO$_4$/C (b) LiFe(PO$_4$)$_{0.9}$F$_{0.3}$/C.

a result of the decomposing reaction, which will then cause the dissolution of iron from the cathode material. The fully F-substitution of LiFe(PO$_4$)$_{0.9}$F$_{0.3}$/C may alleviate the iron dissolution, thus cause a longer cycling life of this material. However, more investigation work is required to clearly explain the real role of fluorine in the crystal structure of lithium ion phosphate.

4. Conclusion

In this study, F-substituted LiFe(PO$_4$)$_{1-x}$F$_{3x}$/C (x: 0, 0.025, 0.05, 0.1) materials were synthesized via a ball milling method by adding LiF to the starting materials of LiFePO$_4$/C. XRD and XPS analyses indicate that F-substitution did not alter the crystal structure of LiFePO$_4$ phase. The LiFe(PO$_4$)$_{0.9}$F$_{0.3}$/C was slightly over substituted with some free LiF remained in the sample. F-substitution can improve the rate capability of these cathode materials. The excessively F-substituted LiFe(PO$_4$)$_{0.9}$F$_{0.3}$/C show the most attractive high rate performance. Its discharge capacity at 10 C rate was 110 mAh g^{-1} with a flat discharge voltage plateau of 3.31–3.0 V versus Li$^+$/Li. The LiFe(PO$_4$)$_{0.9}$F$_{0.3}$/C sample also showed obviously better cycling life at high temperature than the other samples.

clarify the effect of F-substitution on the cycling performance of LiFe(PO$_4$)$_{0.9}$F$_{0.3}$/C sample at elevated temperature, voltage profiles from cycles 10, 100, 200 and 300 at 55 °C for the cells of Li|LiFePO$_4$/C and Li|LiFe(PO$_4$)$_{0.9}$F$_{0.3}$/C are compared in Fig. 9. It is clear that the charge–discharge profiles for LiFe(PO$_4$)$_{0.9}$F$_{0.3}$/C maintained almost the same shape up to the 200th cycle. However, the profiles for un-substituted LiFePO$_4$/C show significant polarization after 100 cycles and the voltage polarization turned to be more severe as cycling proceeded. In addition, decrease of initial discharge voltage was also observed as cycle number increased for Li|LiFePO$_4$/C cell. All these results indicate an increase in cell impedance during cycling, which resulted in a decrease of charge–discharge capacity. The comparison of the charge–discharge profiles at elevated temperature indicated that the F-substitution in LiFe(PO$_4$)$_{0.9}$F$_{0.3}$/C could reduce both the ohmic resistance and lithium diffusion resistance in the cathode material. Fully F-substitution on LiFe(PO$_4$)$_{0.9}$F$_{0.3}$/C has a positive effect to improve the cycle stability at elevated temperature. There are many possible reasons for capacity fading in lithium batteries [25,26], such as the fatigue of crystal structure for the active materials, the loss of electronic contacting among material particles and the decomposition of the electrolyte (which will be accelerated at higher temperature) during cycling. For the difference on cycling behavior between LiFePO$_4$/C and LiFe(PO$_4$)$_{0.9}$F$_{0.3}$/C cathodes, the explaining maybe as following: At elevated temperature, the decomposition of the electrolyte was accelerated and more HF will be generated as

References

[1] A.K. Padhi, K.S. Nanjundaswamy, J.B. Goodenough, J. Electrochem. Soc. 144 (1997) 1189.
[2] A.S. Andersson, B. Kalska, L. Haggstrom, J.O. Thomas, Solid State Ionics 130 (2000) 41.
[3] S.Y. Chung, J.T. Bloking, Y.-M. Chiang, Nat. Mater. 1 (2002) 123.
[4] A. Yamada, S.C. Chung, K. Hinokuma, J. Electrochem. Soc. 148 (2001) A224.
[5] P.P. Prosini, M. Carewska, S. Scaccia, P. Wisniewski, S. Passerini, M. Pasquali, J. Electrochem. Soc. 149 (2002) A886.
[6] M. Takahashi, S. Tobishima, K. Takei, Y. Sakurai, J. Power Sources 97–98 (2001) 508.
[7] N. Ravet, J.B. Goodenough, S. Besner, M. Simoneau, P. Hovington, M. Armand, Proceedings of the 196th ECS Meeting, Hawaii, 17–22 October, 1999.
[8] S.F. Yang, P.Y. Zavalij, M.S. Whittingham, Electrochem. Commun. 3 (2001) 505.
[9] J. Barker, M.Y. Saide, J.L. Swoyer, Electrochem. Solid-State Lett. 6 (2003) A53.
[10] R. Dominko, M. Bele, M. Gaberscek, M. Remskar, D. Hanzel, S. Pejovnikand, J. Jamnik, J. Electrochem. Soc. 152 (2005) A607.
[11] Z. Chen, J.R. Dahn, J. Electrochem. Soc. 149 (2002) A1184.
[12] X.Z. Liao, Z.F. Ma, Y.S. He, X.M. Zhang, L. Wang, Y. Jiang, J. Electrochem. Soc. 152 (2005) A1969.
[13] X.Z. Liao, Z.F. Ma, L. Wang, X.M. Zhang, Y. Jiang, Y.S. He, Electrochem. Solid-State Lett. 7 (2004) A522.

[14] S. Yonezawa, M. Yamasaki, M. Takashima, J. Fluorine Chem. 125 (2004) 1657.

[15] X. Wu, X. Zong, Q. Yang, Z. Jin, H. Wu, J. Fluorine Chem. 107 (2001) 39.

[16] K. Kubo, M. Fujiwara, S. Yamada, S. Arai, M. Kanda, J. Power Sources 68 (1997) 553.

[17] K. Kubo, S. Arai, S. Yamada, M. Kanda, J. Power Sources 81–82 (1999) 599.

[18] T. Ohzuku, A. Ueda, M. Kouguchi, J. Electrochem. Soc. 12 (1995) 4033.

[19] A.R. Naghash, LeeF J.Y., Electrochim. Acta 46 (2001) 2293.

[20] G.-H. Kim, S.-T. Myung, H.J. Bang, Jai Prakash, Y.-K. Sun, Electrochem. Solid-State Lett. 7 (2004) A477.

[21] G.-H. Kim, J.-H. Kim, S.-T. Myung, C.S. Yoon, Y.-K. Suna, J. Electrochem. Soc. 152 (2005) A1707.

[22] H.-S. Shin, S.-H. Park, C.S. Yoon, Y.-K. Sun, Electrochem. Solid-State Lett. 8 (2005) A559.

[23] G.G. Amatucci, N. Pereira, T. Zheng, J.-M. Tarascon, J. Electrochem. Soc. 148 (2001) A171.

[24] J. Barker, M.Y. Saidi, J.L. Swoyera, J. Electrochem. Soc. 150 (2003) A1394.

[25] X. Zhang, P.N. Ross Jr., R. Kostecki, F. Kong, S. Sloop, J.B. Kerr, K.A. Striebel, E.J. Cairns, F. McLarnon, J. Electrochem. Soc. 148 (2001) A463.

[26] J. Shim, R. Kostecki, T. Richardson, X. Song, K.A. Striebel, J. Power Sources 112 (2002) 222.